

# Symbol-Level Precoding for Integrated Sensing and Communications: A Faster-Than-Nyquist Approach

Zihan Liao, Fan Liu, *Member, IEEE*

**Abstract**—In this paper, we propose a novel symbol-level precoding (SLP) method for a multi-user multi-input multi-output (MU-MIMO) downlink Integrated Sensing and Communications (ISAC) system based on the faster-than-Nyquist (FTN) signaling, where an ISAC signal is designed to simultaneously accomplish target sensing and wireless communication tasks. In particular, we minimize the minimum mean squared error (MMSE) for target parameter estimation, while guaranteeing the per-user quality-of-service by exploiting both multi-user and inter-symbol interference with constructive interference (CI) techniques. While the formulated problem is non-convex in general, we propose an efficient successive convex approximation (SCA) method, which solves a convex second-order cone program (SOCP) subproblem at each iteration. Numerical results demonstrate the effectiveness of the proposed FTN-ISAC-SLP design, showing that our method significantly outperforms conventional benchmark approaches in terms of both communication and sensing performance.

**Index Terms**—ISAC, faster-than-nyquist, constructive interference, symbol-level precoding

## I. INTRODUCTION

INTEGRATED sensing and communications (ISAC) has been recognized as a key enabling technology for next-generation wireless networks (such as 5G-Advanced (5G-A) and 6G). It pursues a deep integration between sensing and communication (S&C) such that the two functionalities can be co-designed to improve the hardware-, spectral-, and energy-efficiency, as well as to acquire mutual performance gains [1].

There have been numerous waveform design schemes for ISAC, which may be categorized as two main methodologies, i.e., non-overlapped resource allocation and fully unified waveform design. The first scheme aims to allocate orthogonal/non-overlapped wireless resources to S&C, such that they do not interfere with each other. Nevertheless, this method suffers from poor resource efficiency. As a consequence, it is more favorable to design a fully unified ISAC waveform through the shared use of wireless resources between S&C. In general, fully unified waveform design follows one of the following three schemes: Sensing-centric design (SCD), communication-centric design (CCD), and joint design (JD) [2]. The first two schemes guarantee the priority of sensing/communication capabilities of the ISAC system, while treating the other functionality as a by-product. In contrast to SCD and CCD, JD schemes aim to design an ISAC signal from the ground-up instead of relying on existing S&C waveforms, which leads to a scalable tradeoff between S&C [3].

While the existing JD schemes are well-designed by sophisticated approaches, they generally assume Nyquist pulse shaping in an implicit manner. To further boost the communication throughput under critical sensing constraints, one may consider to leverage the faster-than-Nyquist (FTN) signaling

in the ISAC waveform design. The key idea of FTN signaling is to improve data rate by accelerating the transmitted pulses in the temporal dimension, thus violating the Nyquist criterion and compromising controllable inter-symbol interference (ISI) [4]. For an MU-MIMO system employing FTN signaling, interference appears in both spatial and temporal domains, namely, the multi-user interference (MUI), and the ISI due to non-orthogonal pulse shaping. Conventional precoding designs address the interference issues via channel equalization techniques, e.g., zero forcing, which however ignore the fact that both categories of interference is known to the ISAC base station (BS), and may be leveraged to enhance the useful signal power [5]. The flexibility of JD-based ISAC waveform design allows us to perform symbol level precoding (SLP) to exploit the constructive interference (CI), where transmitted signals are designed based on the knowledge of both the channel state information (CSI) and data information. Different from the conventional block-level precoding relying only on the CSI, the aim of SLP is not to cancel the interference, but rather to control it to impose constructive effect on each information-carrying symbol, thus to improve the communication signal-to-interference-plus-noise ratio (SINR) [6].

In this paper, we propose a novel ISAC precoding technique referred to as FTN-ISAC-SLP. It merges the strategies discussed above, thus gleaning performance improvement for S&C from both temporal and spatial dimensions. We first introduce the system model and performance metrics for the considered MU-MIMO ISAC system employing FTN signaling, and then formulate the ISAC precoding design into an optimization problem. While the problem is non-convex in general, we propose a tailor-made successive convex approximation (SCA) method, which finds a near-optimal solution in polynomial time. Numerical results show that the proposed FTN-ISAC-SLP method achieves significant performance gain in terms of both S&C compared to conventional Nyquist signaling and block-level precoding approaches.

## II. SYSTEM MODEL

We consider a narrowband MIMO ISAC BS equipped with  $N_t$  transmit antennas and  $N_r$  receive antennas, which is serving  $K$  downlink single-antenna users while detecting targets as a monostatic radar. Without loss of generality, we assume  $K < N_t$ . Before formulating the FTN-ISAC-SLP problem, we first elaborate on the system model and performance metrics of both radar sensing and communications.

### A. Signal Model

Let  $\mathbf{S} = [\mathbf{s}_1, \mathbf{s}_2, \dots, \mathbf{s}_K]^T \in \mathbb{C}^{K \times L}$  denote the symbol matrix to be transmitted, with  $\mathbf{s}_k$  being the data stream

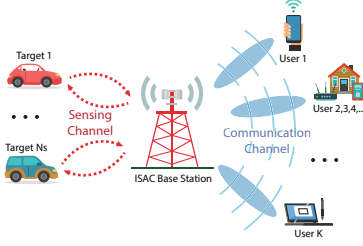


Fig. 1. ISAC Downlink System

intended for the  $k$ -th user with a block length  $L$ , and each entry being drawn from a given constellation. Unless otherwise specified, in this paper we consider a PSK constellation, since the extension to QAM constellations is straightforward [6]. Moreover, let  $\mathbf{X} = [\mathbf{x}_1, \mathbf{x}_2, \dots, \mathbf{x}_{N_t}]^T \in \mathbb{C}^{N_t \times L}$  be the precoded signal matrix, with  $\mathbf{x}_n$  representing the data stream to be transmitted at the  $n$ -th antenna. Suppose that the precoded symbols  $\mathbf{x}_i$  are passed through a root-raised-cosine (RRC) shaping filter  $\varphi(t)$  with a roll-off factor  $\alpha$  and a duration  $T_0$ . The band-limited signal is transmitted with an FTM-specific symbol interval  $T = \tau T_0$  where  $\tau \in [0, 1]$ . Under such a setting, the transmit FTM signal  $x_n(t)$  can be expressed as

$$x_n(t) = \sum_{i=0}^{L-1} x_{n,i} \varphi(t - iT), \quad (1)$$

where  $x_{n,i}$  represents the  $i$ -th element of  $\mathbf{x}_n$ .

1) *Communication Model:* Consider the quasi-static flat fading channel matrix  $\mathbf{H}_C = [\mathbf{h}_1^C, \mathbf{h}_2^C, \dots, \mathbf{h}_K^C]^T \in \mathbb{C}^{K \times N_t}$  that models the MUI among different data streams, where  $\mathbf{h}_k^C$  is the channel vector of  $k$ -th user. Then the received signal at the  $k$ -th user can be expressed as

$$r_k^C(t) = \sum_{i=0}^{N_t-1} h_{k,i}^C x_i(t) + n_k^C(t), \quad (2)$$

where  $h_{k,i}^C$  represents the  $i$ -th elements of  $\mathbf{h}_{C,k}$  and  $n_k^C(t)$  is the complex-valued additive white Gaussian noise (AWGN) at the  $k$ -th user with zero mean and variance  $\sigma_C^2$ .

The received FTM signal after passing through a matched filter  $\varphi^*(-t)$  at the  $k$ -th user is given by

$$\begin{aligned} y_k^C(t) &= r_k^C(t) * \varphi^*(-t) \\ &= \sum_{i=0}^{N_t-1} h_{k,i}^C x_i(t) * \varphi^*(-t) + n_k^C(t) * \varphi^*(-t) \\ &= \sum_{i=0}^{N_t-1} \sum_{j=0}^{L-1} h_{k,i}^C x_{i,j} \phi(t - jT) + \eta_k(t), \end{aligned} \quad (3)$$

where

$$\begin{aligned} \phi(t) &= \int_{-\infty}^{\infty} \varphi(\zeta) \varphi^*(\zeta - t) d\zeta, \\ \eta_k(t) &= \int_{-\infty}^{\infty} n_k^C(\zeta) \varphi^*(\zeta - t) d\zeta. \end{aligned} \quad (4)$$

The  $l$ -th filtered sample at the  $k$ -th user  $y_{k,l} = y_k(lT)$  ( $l = 0, 1, \dots, L-1$ ) can be expressed as

$$y_{k,l}^C = \sum_{i=0}^{N_t-1} \sum_{j=0}^{L-1} h_{k,i}^C x_{i,j} \phi((l-j)T) + \eta_k(lT), \quad (5)$$

which can be written in a compact matrix form as

$$\tilde{\mathbf{Y}}_C = \mathbf{H}_C \mathbf{X} \Phi + \tilde{\mathbf{N}}_C, \quad (6)$$

where  $\tilde{\mathbf{Y}}_C = (y_{k,l}) \in \mathbb{C}^{K \times L}$ , and  $\Phi \in \mathbb{R}^{L \times L}$  is defined as

$$\Phi = \begin{bmatrix} \phi(0) & \phi(-T) & \dots & \phi(-(L-1)T) \\ \phi(T) & g(0) & \dots & \phi(-(L-2)T) \\ \vdots & \vdots & \ddots & \vdots \\ \phi((L-1)T) & \phi((L-2)T) & \dots & \phi(0) \end{bmatrix}, \quad (7)$$

which is a positive semidefinite Toeplitz symmetric matrix. Moreover,  $\tilde{\mathbf{N}}_C = [\boldsymbol{\eta}_0, \boldsymbol{\eta}_1, \dots, \boldsymbol{\eta}_{K-1}]^T$ , with  $\boldsymbol{\eta}_k = [\eta_k(0), \eta_k(T), \dots, \eta_k((L-1)T)]^T$  being the corresponding noise vector at the  $k$ -th user. Notice that  $\mathbb{E}[\boldsymbol{\eta}_k \boldsymbol{\eta}_k^H] = \sigma_C^2 \Phi$ , which indicates that the noise received at each user is not independent. To decorrelate the noise, consider the eigenvalue decomposition of  $\Phi$  is  $\mathbf{U} \mathbf{\Lambda} \mathbf{U}^H$  where  $\mathbf{U}$  is a unitary matrix containing eigenvectors and  $\mathbf{\Lambda}$  is a diagonal matrix composed by eigenvalues. Right-multiplying  $\mathbf{U}$  at both sides of (6) yields

$$\mathbf{Y}_C = \mathbf{H}_C \mathbf{X} \mathbf{U} \mathbf{\Lambda} + \mathbf{N}_C, \quad (8)$$

where  $\mathbf{Y}_C = \tilde{\mathbf{Y}}_C \mathbf{U}$  and  $\mathbf{N}_C = \tilde{\mathbf{N}}_C \mathbf{U}$ . By doing so, the covariance matrix for row vectors of  $\mathbf{N}_C$  becomes  $\sigma_C^2 \mathbf{\Lambda}$ , i.e., a diagonal matrix.

2) *Radar Sensing Model:* Consider the target response matrix (TRM)  $\mathbf{H}_R = [\mathbf{h}_1^R, \mathbf{h}_2^R, \dots, \mathbf{h}_{N_r}^R]^T \in \mathbb{C}^{N_r \times N_t}$  that models the sensing channel. Depending on the sensing scenarios,  $\mathbf{H}_R$  can be of different forms. For angular extended target model where all the point-like scatterers are located in the same range bin, we have

$$\mathbf{H}_R = \sum_{i=1}^{N_s} \alpha_i \mathbf{b}(\theta_i) \mathbf{a}^H(\theta_i), \quad (9)$$

where  $N_s$  is the number of scatterers,  $\alpha_i$  and  $\theta_i$  denote the reflection coefficient and the angle of the  $i$ -th scatterer, and  $\mathbf{a}(\theta) \in \mathbb{C}^{N_t \times 1}$  and  $\mathbf{b}(\theta) \in \mathbb{C}^{N_r \times 1}$  are transmit and receive steering vectors. Another example is to detect multiple point targets using OFDM waveforms. Suppose that the radar receives echoes from  $N_s$  point targets. Each target has individual reflection coefficient, angle, delay, and Doppler parameters  $\alpha_i$ ,  $\theta_i$ ,  $\tau_i$ , and  $f_{D,i}$ . And  $\Delta f$  and  $T_O$  represent subcarrier spacing and OFDM symbol duration. Then  $\mathbf{H}_R$  can be modeled as a TRM defined on the  $n$ -th subcarrier and the  $m$ -th OFDM symbol as

$$\mathbf{H}_R = \mathbf{H}_{n,m} = \mathbf{B}(\Theta) \mathbf{C}_n \mathbf{D}_m \mathbf{A}^H(\Theta), \quad (10)$$

where

$$\mathbf{A}(\Theta) = [\mathbf{a}(\theta_1), \dots, \mathbf{a}(\theta_{N_s})], \mathbf{B}(\Theta) = [\mathbf{b}(\theta_1), \dots, \mathbf{b}(\theta_{N_s})] \quad (11)$$

are transmit and receive steering matrices, and

$$\begin{aligned} \mathbf{C}_n &= \text{Diag} \left( [\alpha_1 e^{-j2\pi(n-1)\Delta f \tau_1}, \dots, \alpha_{N_s} e^{-j2\pi(n-1)\Delta f \tau_{N_s}}] \right), \\ \mathbf{D}_m &= \text{Diag} \left( [e^{j2\pi f_{D,1}(m-1)T_O}, \dots, e^{j2\pi f_{D,N_s}(m-1)T_O}] \right) \end{aligned} \quad (12)$$

are phase shifting matrices resulted by time delay and Doppler effect of each target.

To guarantee the generality of the proposed method, we consider a generic TRM  $\mathbf{H}_R$  instead of specific models above. Similar to the communication model, the received echo signal at the  $k$ -th receive antenna can be written as

$$y_k^R(t) = \sum_{i=0}^{N_t-1} h_{k,i}^R x_i(t) + n_k^R(t), \quad (13)$$

where  $h_{k,i}^R$  represents the  $i$ -th elements of  $\mathbf{h}_{R,k}$  and  $n_k^R(t)$  is the complex-valued AWGN at the  $k$ -th receive antenna with zero mean and variance  $\sigma_R^2$ . At the sensing receiver, we directly sample the received signal without passing it through the pulse-shaping filter, yielding the following radar received signal model

$$\mathbf{Y}_R = \mathbf{H}_R \mathbf{X} \mathbf{C}^\top + \mathbf{N}_R, \quad (14)$$

where  $\mathbf{N}_R$  denotes an AWGN matrix, with zero mean and the variance of each entry being  $\sigma_R^2$ . Here we assume  $\mathbf{h} = \text{vec}(\mathbf{H}_R) \sim \mathcal{CN}(\mathbf{0}, \sigma_H^2 \mathbf{I})$  and  $\mathbf{C}$  is given by

$$\mathbf{C} = \begin{bmatrix} c_0 & 0 & \cdots & 0 \\ c_1 & c_0 & \ddots & \vdots \\ \vdots & \vdots & \ddots & \vdots \\ c_{P-1} & c_{P-2} & \ddots & 0 \\ 0 & c_{P-1} & \ddots & c_0 \\ \vdots & \vdots & \vdots & \vdots \\ 0 & \cdots & \cdots & c_{P-1} \end{bmatrix}, \quad (15)$$

where  $\mathbf{c} = [c_0, c_1, \dots, c_{P-1}]^\top$  is the sample vector for RRC function  $\varphi(t)$  with sampling number  $P$ .

*Remark:* In the communication model we attempt to detect the signal  $\mathbf{S}$  from  $\mathbf{X}$  in the receiver side, thus we pass the received signal to RRC matched filter to maximize the received SINR for each precoded symbol. In the sensing model our aim is to recover the TRM  $\mathbf{H}_R$  from the raw observation (14), rather than to recover  $\mathbf{X}$ . Therefore, we treat  $\mathbf{X} \mathbf{C}^\top$  as an equivalent transmitted waveform and regard (14) as the sufficient statistics for estimating  $\mathbf{H}_R$ , which needs not to be match-filtered by the RRC pulse.

### B. CI Constraint for Communication

Following the CI constraint given in [7], for any transmitted symbol  $s$  and its corresponding received symbol  $y$  at the receiver side, they must satisfy the following inequality to exploit the CI effect

$$|\Im\{s^* y\}| - \Re\{s^* y\} \tan \theta \leq -\sqrt{\Gamma \sigma^2} \tan \theta, \quad (16)$$

where  $\sigma^2$  is the variance of the noise imposes on this symbol,  $\Gamma$  is the required SNR and  $\theta$  depends on the modulation type. Let  $\mathbf{Y}_C = [\mathbf{y}_0, \mathbf{y}_1, \dots, \mathbf{y}_{K-1}]^\top$  and  $\boldsymbol{\sigma} = \sqrt{\text{diag}(\sigma_C^2 \boldsymbol{\Lambda})} = [\sigma_C \Lambda_{0,0}, \sigma_C \Lambda_{1,1}, \dots, \sigma_C \Lambda_{L-1,L-1}]^\top$  where  $\text{diag}$  refers to the operation taking the entries in the diagonal and stacking them

as a vector. Then the CI constraint for the  $k$ -th user can be written as

$$|\Im\{\mathbf{s}_k^* \circ \mathbf{y}_k\}| - \Re\{\mathbf{s}_k^* \circ \mathbf{y}_k\} \tan \theta \leq (-\sqrt{\Gamma_k} \tan \theta) \boldsymbol{\sigma}, \quad \forall k, \quad (17)$$

where  $\Gamma_k$  is the required SINR of the  $k$ -th user, and  $\circ$  refers to the Hadamard product. For the received symbol at the  $k$ -th user we have

$$\mathbf{y}_k^\top = \mathbf{h}_k^{C^\top} \mathbf{X} \mathbf{U} \boldsymbol{\Lambda}. \quad (18)$$

By noting the fact that  $\mathbf{s}_k^* \circ \mathbf{y}_k$  can be equivalently expressed as  $\mathbf{S}_k^* \mathbf{y}_k = \mathbf{S}_k^* \mathbf{y}_k$ , where

$$\mathbf{S}_k = \text{Diag}(\mathbf{s}_k) = \begin{bmatrix} e^{j\phi_{k,0}} & 0 & \cdots & 0 \\ 0 & e^{j\phi_{k,1}} & \cdots & 0 \\ \vdots & \vdots & \ddots & \vdots \\ 0 & 0 & \cdots & e^{j\phi_{k,L-1}} \end{bmatrix}, \quad (19)$$

the inequality (17) can be recast to

$$\begin{aligned} \left| \Im\{\mathbf{h}_k^{C^\top} \mathbf{X} \mathbf{U} \boldsymbol{\Lambda} \mathbf{S}_k^*\} \right| - \Re\{\mathbf{h}_k^{C^\top} \mathbf{X} \mathbf{U} \boldsymbol{\Lambda} \mathbf{S}_k^*\} \tan \theta \\ \leq (-\sqrt{\Gamma_k} \tan \theta) \boldsymbol{\sigma}^\top, \quad \forall k, \end{aligned} \quad (20)$$

which is a linear constraint in  $\mathbf{X}$  and is thus convex.

### C. MMSE for Radar Sensing

Let  $\mathbf{y}_R = \text{vec}(\mathbf{Y}_R)$ ,  $\mathbf{h}_R = \text{vec}(\mathbf{H}_R)$  and  $\mathbf{n}_R = \text{vec}(\mathbf{N}_R)$ . Equation (14) can be expanded as

$$\mathbf{y}_R = (\mathbf{C} \mathbf{X}^\top \otimes \mathbf{I}_{N_r}) \mathbf{h}_R + \mathbf{n}_R. \quad (21)$$

According to [8], the corresponding MMSE for estimating  $\mathbf{h}_R$  from the noisy observation  $\mathbf{y}_R$  is

$$\begin{aligned} \text{MMSE} &= \mathbb{E}(\|\mathbf{h}_R - \mathbf{h}_R^{\text{MMSE}}\|_2^2) \\ &= \text{tr} \left( (\sigma_H^{-2} \mathbf{I} + \sigma_R^{-2} (\mathbf{C} \mathbf{X}^\top \otimes \mathbf{I}_{N_r})^H (\mathbf{C} \mathbf{X}^\top \otimes \mathbf{I}_{N_r}))^{-1} \right) \\ &= \text{tr} \left( (\sigma_H^{-2} \mathbf{I} + \sigma_R^{-2} (\mathbf{X}^* \mathbf{C}^\top \mathbf{C} \mathbf{X}^\top \otimes \mathbf{I}_{N_r}))^{-1} \right) \\ &= \sigma_R^2 N_r \text{tr} \left( \left( \frac{\sigma_R^2}{\sigma_H^2} \mathbf{I} + \mathbf{X} \boldsymbol{\Psi} \mathbf{X}^H \right)^{-1} \right), \end{aligned} \quad (22)$$

where  $\boldsymbol{\Psi} = \mathbf{C}^\top \mathbf{C}$ . Notice that this expression is non-convex in  $\mathbf{X}$ , which will be tackled in the next section.

## III. FTN-ISAC SYMBOL-LEVEL PRECODING

### A. Problem Formulation

Based on the discussion above, the precoding optimization problem can be expressed as

$$\begin{aligned} \min_{\mathbf{X}} f(\mathbf{X}) &= \text{tr} \left( \left( \frac{\sigma_R^2}{\sigma_H^2} \mathbf{I} + \mathbf{X} \boldsymbol{\Psi} \mathbf{X}^H \right)^{-1} \right) \\ \text{s.t.} \quad & \left| \Im\{\mathbf{h}_k^{C^\top} \mathbf{X} \mathbf{U} \boldsymbol{\Lambda} \mathbf{S}_k^*\} \right| - \Re\{\mathbf{h}_k^{C^\top} \mathbf{X} \mathbf{U} \boldsymbol{\Lambda} \mathbf{S}_k^*\} \tan \theta \\ & \leq (-\sqrt{\Gamma_k} \tan \theta) \boldsymbol{\sigma}^\top, \quad \forall k, \end{aligned} \quad (23)$$

$$\|\mathbf{X} \mathbf{C}^\top\|_F^2 \leq E.$$

That is, we design the precoded symbol matrix  $\mathbf{X}$  for the to-be-transmitted symbol matrix  $\mathbf{S}$ , such that the MMSE for radar sensing is minimized while guaranteeing the CI conditions for communication under a given energy budget  $E$ .

### B. Lower-Bound for the MMSE

We first derive the lower bound of problem (23) by considering the following optimization problem that solely minimizes the MMSE without imposing CI constraints

$$\min_{\mathbf{X}} f(\mathbf{X}) = \text{tr} \left( \left( \frac{\sigma_R^2}{\sigma_H^2} \mathbf{I} + \mathbf{X} \mathbf{\Psi} \mathbf{X}^H \right)^{-1} \right) \quad \text{s.t.} \|\mathbf{X} \mathbf{C}^\top\|_F^2 \leq E. \quad (24)$$

By letting  $\tilde{\mathbf{X}} = \mathbf{X} \mathbf{C}^\top$ , problem (24) can be recast to

$$\min_{\tilde{\mathbf{X}}} f(\tilde{\mathbf{X}}) = \text{tr} \left( \left( \frac{\sigma_R^2}{\sigma_H^2} \mathbf{I} + \tilde{\mathbf{X}} \tilde{\mathbf{X}}^H \right)^{-1} \right) \quad \text{s.t.} \|\tilde{\mathbf{X}}\|_F^2 \leq E \quad (25)$$

which is independent of  $\tau$ . According to [9], the optimal value of problem (25) is

$$f_{\min} = \sum_{i=1}^{N_t} \frac{1}{\lambda_i^2 + \frac{\sigma_R^2}{\sigma_H^2}}, \quad (26)$$

where  $\lambda_i^2 = \left( \kappa - \frac{\sigma_R^2}{\sigma_H^2} \right)^+$  and  $a^+ = \max(a, 0)$ . The constant  $\kappa$  is chosen to satisfy  $\sum_{i=1}^{N_t} \lambda_i^2 = E$ .

### C. SCA Algorithm for Solving Problem (23)

It can be readily observed that the feasible region  $\mathcal{Q}$  for (23) is convex, whereas the objective function is not. To address this issue, we propose an SCA algorithm to solve problem (23) in an iterative manner.

To proceed with the SCA algorithm, we approximate  $f(\mathbf{X})$  using its first-order Taylor expansion near a given point  $\mathbf{X}_i \in \mathcal{Q}$  as

$$f(\mathbf{X}) \approx f(\mathbf{X}_i) + \Re \left\{ \text{tr} \left( \nabla f(\mathbf{X}_i)^H (\mathbf{X} - \mathbf{X}_i) \right) \right\} \quad (27)$$

where  $\nabla f(\cdot)$  represents the gradient of  $f(\cdot)$  and  $\nabla f(\mathbf{X}_i)$  can be calculated as

$$\begin{aligned} \nabla f(\mathbf{X}_i) = & -2 \left( \frac{\sigma_R^2}{\sigma_H^2} \mathbf{I} + \mathbf{X}_i \mathbf{\Psi} \mathbf{X}_i^H \right)^{-1} \left( \frac{\sigma_R^2}{\sigma_H^2} \mathbf{I} + \mathbf{X}_i \mathbf{\Psi} \mathbf{X}_i^H \right)^{-1} \mathbf{X}_i \mathbf{\Psi} \\ & (28) \end{aligned}$$

At the  $(i+1)$ -th iteration of the SCA algorithm, we solve the following convex optimization problem

$$\begin{aligned} \min_{\mathbf{X}} g(\mathbf{X}) = & \Re \left\{ \text{tr} \left( \nabla f(\mathbf{X}_i)^H (\mathbf{X} - \mathbf{X}_i) \right) \right\} \\ \text{s.t.} \quad & \left| \Im \left\{ \mathbf{h}_k^{C^\top} \mathbf{X} \mathbf{U} \mathbf{\Lambda} \mathbf{S}_k^* \right\} \right| - \Re \left\{ \mathbf{h}_k^{C^\top} \mathbf{X} \mathbf{U} \mathbf{\Lambda} \mathbf{S}_k^* \right\} \tan \theta \\ & \leq (-\sqrt{\Gamma_k} \tan \theta) \sigma^\top, \forall k, \end{aligned} \quad (29)$$

$$\|\mathbf{X} \mathbf{C}^\top\|_F^2 \leq E,$$

where  $\mathbf{X}_i \in \mathcal{Q}$  is the  $i$ -th iterative point. By solving the convex problem (29) we get a solution  $\mathbf{X}^* \in \mathcal{Q}$ . Note that  $g(\mathbf{X}^*) \leq g(\mathbf{X}_i) = 0$ , indicating that  $\mathbf{X}^* - \mathbf{X}_i$  yields a descent direction for the objective function. With a properly chosen step size  $t \in [0, 1]$ , one may get the  $(i+1)$ -th iteration point as

$$\mathbf{X}_{i+1} = \mathbf{X}_i + t(\mathbf{X}^* - \mathbf{X}_i) = (1-t)\mathbf{X}_i + t\mathbf{X}^*. \quad (30)$$

Since  $\mathbf{X}_i, \mathbf{X}^* \in \mathcal{Q}$  by the definition of convexity, we have  $\mathbf{X}_{i+1} \in \mathcal{Q}$ , which is a feasible solution to problem (23).

We are now ready to present Algorithm 1 to solve problem (29) based on the discussion above.

---

### Algorithm 1 SCA Algorithm for Solving (23)

---

**Require:**  $\mathbf{H}, \mathbf{\Psi}, E, \mathbf{S}, \sigma, \Gamma_k, \forall k$ , the execution threshold  $\epsilon$  and the maximum iteration number  $i_{\max}$ .

**Ensure:**  $\mathbf{X}^*$

- 1: initialize  $\mathbf{X}_0 \in \mathcal{Q}$  by picking up  $\mathbf{X}_{-1}$  randomly and solving problem (29),  $i = 0$ .
  - 2: **repeat**
  - 3:   Calculate the gradient  $\nabla f(\mathbf{X}_i)$  by equation (28).
  - 4:   Solve problem (29) to obtain  $\mathbf{X}^*$ .
  - 5:   Update the solution by  $\mathbf{X}_{i+1} = \mathbf{X}_i + t(\mathbf{X}^* - \mathbf{X}_i)$ , where  $t$  is determined by using the exact line search.
  - 6:    $i = i + 1$ .
  - 7: **until**  $\|\mathbf{X}_i - \mathbf{X}_{i-1}\|_F^2 \leq \epsilon$  or  $i = i_{\max}$ .
  - 8:  $\mathbf{X}^* = \mathbf{X}_i$
- 

## IV. NUMERICAL RESULTS

In this section, we provide numerical results to verify the superiority of the proposed FTN-ISAC-SLP approaches. Without loss of generality, we consider an ISAC BS that is equipped with  $N_t = 16$  and  $N_r = 20$  antennas for its transmitter and receiver. The noise variances are set as  $\sigma_C^2 = \sigma_R^2 = 0$  dBm, and the frames length is set as  $L = 30$ . The variance of the fluctuation of TRM is set as  $\sigma_H^2 = 20$  dBm. Without loss of generality, all the communication users are imposed with the same worst-case QoS, i.e.,  $\Gamma_k = \Gamma, \forall k$ .

Our baseline ISAC-BLP is the ISAC beamforming method from [10], namely the block-level precoding method to find the optimal linear precoding matrix  $\mathbf{W}_{DF}$  that minimizes the sensing CRB with guaranteed per-user SINR, through solving the problem below.

$$\begin{aligned} \min_{\mathbf{W}_{DF}} \text{MMSE}(\mathbf{W}_{DF}) = & \frac{\sigma_R^2 N_r}{L} \left( \left( \frac{\sigma_R^2}{\sigma_H^2} \mathbf{I} + \mathbf{W}_{DF} \mathbf{W}_{DF}^H \right)^{-1} \right) \\ \text{s.t.} \quad & \gamma_k \geq \Gamma_k, \forall k, L \|\mathbf{W}_{DF}\|_F^2 \leq E. \end{aligned} \quad (31)$$

where  $\gamma_k$  is the SINR at  $k$ -th user. In order to ensure a fair comparison, we replace the original objective function CRB in [10] with the MMSE.

Fig. 2 shows the convergence performance of the proposed SCA algorithm. The tolerance threshold of the algorithm is set as  $\epsilon = 10^{-4}$ . The algorithm converges and approaches to the lower bound we derived in above section. It can be observed that the proposed FTN-ISAC-SLP method outperforms the benchmark block-level design.

Fig. 3 shows the constellation plots for both the ISAC-BLP and FTN-ISAC-SLP approaches. The green points depict the region for SINR constraint while the blue points depict the region for CI constraint. It is clearly observed that the resulting CI constellation gearnearly yields larger SNR compared to the block-level precoding.

In Fig. 4, we show the communication throughput performance with increased SNR threshold. Suppose the number of successfully recovered bits are  $N_b$ , our throughput is calculated by  $N_b/\tau$  per time unit. We set FTN duration factor  $\tau = 0.8, 0.9$  and 1 respectively, and for ISAC-BLP  $\tau = 1$ . As  $\tau$  decreases, the throughput increases. When  $\tau = 1$ ,



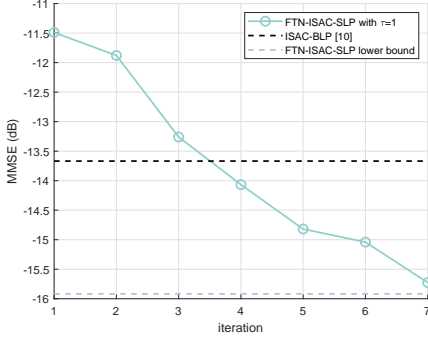


Fig. 2. MMSE versus SCA iteration in case of  $K = 12$ ,  $\Gamma = 15$  dB,  $E = 40$  dBm.

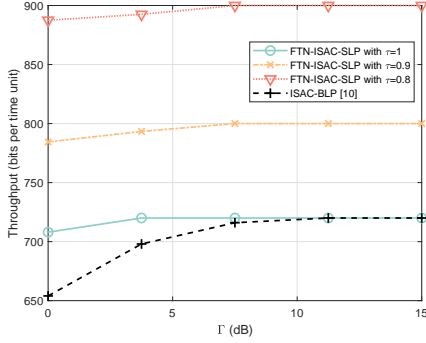


Fig. 4. Throughput versus SNR in the case of  $K = 12$ ,  $E = 40$  dBm.

$T = T_0$ , the FTN signaling reduces to Nyquist pulse shaping, whereas it still outperforms the ISAC-BLP method thanks to the exploitation of the CI effect.

Finally in Fig. 5, we show the radar estimation MMSE with increased SNR threshold for communication users. It is observed that when the communications SNR is on the rise, the estimation performance becomes worse, which indicates that there is an inherent tradeoff between communication and sensing performance. An increasing trend of MMSE when  $\tau$  increases is observed, because the power constraint  $\|\mathbf{X}\mathbf{C}^T\|_F^2 \leq E$  is tightened as  $\tau$  increases. Again, our results show the superiority of the proposed FTN-ISAC-SLP method over that of the ISAC-BLP due to leveraging the CI constraint.

## V. CONCLUSION

This paper studies symbol-level precoding for faster-than-Nyquist signaling in ISAC, where a precoded symbol matrix is developed to carry out target sensing and information signaling simultaneously. In particular, we guarantee the per-user constructive interference constraint in the downlink while minimizing the MMSE for target estimation. Despite the non-convexity of the formulated precoding problem, we design an effective successive convex approximation method that, at each iteration, resolves a second-order cone program subproblem. The superiority of the proposed FTN-ISAC-SLP method is demonstrated by numerical results, which show that our method is capable of greatly enhancing both communication and sensing performance compared to conventional block-level precoding based on Nyquist pulse shaping.

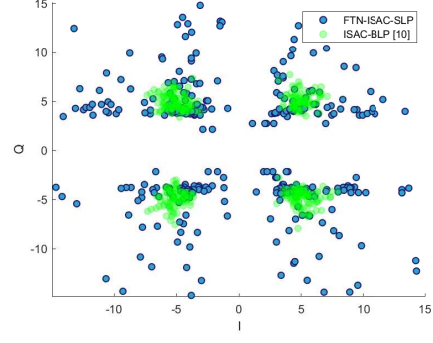


Fig. 3. Constellation plot of the received symbols in case of  $K = 12$ ,  $\Gamma = 15$  dB,  $E = 35$  dBm.

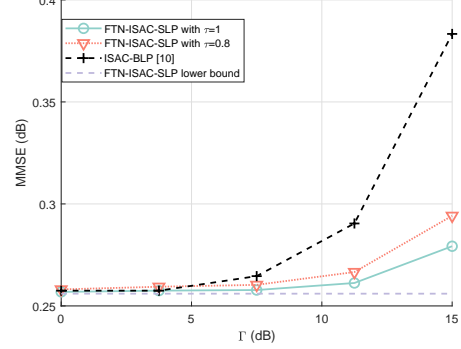


Fig. 5. MMSE versus SNR, in the case of  $K = 8$ ,  $E = 30$  dBm.

## REFERENCES

- [1] D. K. Pin Tan, J. He, Y. Li, A. Bayesteh, Y. Chen, P. Zhu, and W. Tong, "Integrated sensing and communication in 6G: Motivations, use cases, requirements, challenges and future directions," in *2021 1st IEEE International Online Symposium on Joint Communications & Sensing (JC&S)*, 2021, pp. 1–6.
- [2] F. Liu, Y. Cui, C. Masouros, J. Xu, T. X. Han, Y. C. Eldar, and S. Buzzi, "Integrated sensing and communications: Toward dual-functional wireless networks for 6G and beyond," *IEEE Journal on Selected Areas in Communications*, vol. 40, no. 6, pp. 1728–1767, 2022.
- [3] Z. Feng, Z. Fang, Z. Wei, X. Chen, Z. Quan, and D. Ji, "Joint radar and communication: A survey," *China Communications*, vol. 17, no. 1, pp. 1–27, 2020.
- [4] J. B. Anderson, F. Rusek, and V. Öwall, "Faster-than-Nyquist signaling," *Proceedings of the IEEE*, vol. 101, no. 8, pp. 1817–1830, 2013.
- [5] D. Spano, M. Alodeh, S. Chatzinotas, and B. Ottersten, "Faster-than-Nyquist signaling through spatio-temporal symbol-level precoding for the multiuser mimo downlink channel," *IEEE Transactions on Wireless Communications*, vol. 17, no. 9, pp. 5915–5928, 2018.
- [6] A. Li, D. Spano, J. Krivochiza, S. Domouchtsidis, C. G. Tsinos, C. Masouros, S. Chatzinotas, Y. Li, B. Vucetic, and B. Ottersten, "A tutorial on interference exploitation via symbol-level precoding: Overview, state-of-the-art and future directions," *IEEE Communications Surveys & Tutorials*, vol. 22, no. 2, pp. 796–839, 2020.
- [7] C. Masouros and G. Zheng, "Exploiting known interference as green signal power for downlink beamforming optimization," *IEEE Transactions on Signal Processing*, vol. 63, no. 14, pp. 3628–3640, 2015.
- [8] S. M. Kay, *Fundamentals of statistical signal processing: estimation theory*. Prentice-Hall, Inc., 1993.
- [9] Y. Yang and R. S. Blum, "MIMO radar waveform design based on mutual information and minimum mean-square error estimation," *IEEE Transactions on Aerospace and Electronic Systems*, vol. 43, no. 1, pp. 330–343, 2007.
- [10] F. Liu, Y.-F. Liu, A. Li, C. Masouros, and Y. C. Eldar, "Cramér-Rao bound optimization for joint radar-communication beamforming," *IEEE Transactions on Signal Processing*, vol. 70, pp. 240–253, 2022.